BJR

Received: 8 May 2014 | Revised: 29 July 2014 | Accepted: 15 September 2014

doi: 10.1259/bjr.20140342

Cite this article as:
Park JM, Park S-Y, Ye S-J, Kim JH, Carlson J, Wu H-G. New conformity indices based on the calculation of distances between the target volume and the volume of reference isodose. Br J Radiol 2014;87:20140342.

FULL PAPER

New conformity indices based on the calculation of distances between the target volume and the volume of reference isodose

[1,2,3,4]J M PARK, PhD, [1,2,3,5]S-Y PARK, MS, [1,2,3,6]S-J YE, PhD, [1,2,3]J H KIM, MD, [6]J CARLSON, BS and [1,2,3,7]H-G WU, MD

[1]Department of Radiation Oncology, Seoul National University Hospital, Seoul, Republic of Korea
[2]Institute of Radiation Medicine, Seoul National University Medical Research Center, Seoul, Republic of Korea
[3]Biomedical Research Institute, Seoul National University College of Medicine, Seoul, Republic of Korea
[4]Center for Convergence Research on Robotics, Advance Institutes of Convergence Technology, Suwon, Republic of Korea
[5]Interdiciplinary Program in Radiation Applied Life Science, Seoul National University College of Medicine, Seoul, Republic of Korea
[6]Program in Biomedical Radiation Sciences, Department of Transdisciplinary Studies, Seoul National University Graduate School of Convergence Science and Technology, Suwon, Republic of Korea
[7]Department of Radiation Oncology, Seoul National University College of Medicine, Seoul, Republic of Korea

Address correspondence to: Mr H-G Wu
E-mail: wuhg@snu.ac.kr

Objective: To present conformity indices (CIs) based on the distance differences between the target volume (TV) and the volume of reference isodose (V_{RI}).
Methods: The points on the three-dimensional surfaces of the TV and the V_{RI} were generated. Then, the averaged distances between the points on the TV and the V_{RI} were calculated ($CI_{distance}$). The performance of the presented CIs were evaluated by analysing six situations, which were a perfect match, an expansion and a reduction of the distance from the centroid to the V_{RI} compared with the distance from the centroid to the TV by 10%, a lateral shift of the V_{RI} by 3 cm, a rotation of the V_{RI} by 45° and a spherical-shaped V_{RI} having the same volume as the TV. The presented CIs were applied to the clinical prostate and head and neck (H&N) plans.
Results: For the perfect match, $CI_{distance}$ was 0 with 0 as the standard deviation (SD). When expanding and reducing, $CI_{distance}$ was 10 and −10 with SDs <1.3, respectively. With shifting and rotating of the V_{RI}, the $CI_{distance}$ was almost 0 with SDs >11. The average value of the $CI_{distance}$ in the prostate and H&N plans was 0.13 ± 7.44 and 6.04 ± 23.27, respectively.
Conclusion: The performance of the $CI_{distance}$ was equal or better than those of the conventional CIs.
Advances in knowledge: The evaluation of target conformity by the distances between the surface of the TV and the V_{RI} could be more accurate than evaluation with volume information.

The goal of radiation therapy is the conformal delivery of a prescription dose to whole target volumes (TVs) homogeneously, while minimizing the dose delivered to adjacent normal tissues.[1–4] In order to achieve this goal, various state-of-the-art techniques, such as intensity-modulated radiation therapy and volumetric-modulated arc therapy (VMAT) have gained popularity.[5–12] A tool to compare the quality of different plans in terms of target conformity was required, thus the conformity index (CI) was proposed by the Radiation Therapy Oncology Group (RTOG) in 1993 and described in Report 62 of the International Commission on Radiation Units and Measurements.[13,14]

The CI is an indicator that assesses the degree of congruence between a shape of the reference isodose volume (V_{RI}) and the shape of the TV. Two concepts are included in the CI, which are target coverage and degree of normal tissue sparing in the proximity of the target. Although this could be verified by a manual review of dose distributions calculated on patient CT images slice by slice, detailed comparisons among several treatment plans would be inconvenient.[2] The conformity could also be verified by reviewing dose–volume histograms (DVHs) of each structure calculated by the treatment planning system. Since the pre-requisite of the evaluation with DVHs is the contouring of organs at risk (OARs), healthy tissues crossed by the beam could not be taken into account owing to the difficulties of contouring and the absence of sufficient data concerning the dose–volumetric tolerance information of these tissues.[2] Therefore, a value to quantify the conformity was needed, and various studies on the CI have been performed.

Table 1. Comparison of conformity indices

CI_{RTOG}	$CI_{RTOG}=\frac{V_{RI}}{TV}$	RTOG
CVF	$CVF=\frac{TV_{RI}}{TV}$	SALT group
HTCI	$HTCI=\frac{TV_{RI}}{V_{RI}}$	Lomax and Scheib[16]
Modified HTCI	$\text{Modified HTCI}=\frac{1}{r}\sum_{i=1}^{r}\left(\frac{TV_{RI,i}}{V_{RI,i}}\right)$	Leung et al[17]
CN	$CN=\frac{TV_{RI}}{TV}\times\frac{TV_{RI}}{V_{RI}}$	van't Riet et al[18] and Paddick[19]
COIN	$COIN=CN\times\prod_{i=1}^{N_{CO}}\left(1-\frac{V_{COref,i}}{V_{CO,i}}\right)$	Baltas et al[20]
COSI	$COSI=1-\frac{V(OAR)_{>tol}}{TV_{RI}}$	Menhel et al[21]
CGI	$CGI_C=100\times\frac{TV}{V_{RI}}$	Wagner et al[22]
	$CGI_C=100-\{100\times[(R_{Eff,50\%Rx}-R_{Eff,Rx})-0.3\ \text{cm}]\}$	
	$CGI=\frac{CGI_c+CGI_g}{2}$	
CDI	$CDI=\frac{NT_{RI}+(TV-TV_{RI})}{\frac{1}{2}\times(S_{RI}+S_{TV})}$	Wu et al[25]
DSC	$DSC=\frac{2\times TV_{RI}}{TV+V_{RI}}$	Dice[23]

CDI, conformity distance index; CGI, conformity/gradient index; CI_{RTOG}, conformity index by the Radiation Therapy Oncology Group; CN, conformation number; COIN, conformity index; COSI, critical organ scoring index; CVF, coverage volume factor; DSC, dice similarity coefficient; HTCI, healthy tissue conformity index; N_{CO}, number of OARs; NT_{RI}, normal tissue volume receiving the reference dose or more than the reference dose; OAR, organ at risk; *r*, the number of targets with different reference doses; $R_{Eff,50\%Rx}$, effective radius of the isodose line equal to 50% of the prescription isodose volume; $R_{Eff,Rx}$, effective radius of the prescription isodose volume; RTOG, Radiation Therapy Oncology Group; SALT, Saint-Anne–Lariboisiere–Tenon group; S_{RI}, surfaces of the V_{RI}; S_{TV}, surfaces of the TV; TV, volume of target volume; TV_{RI}, target volume covered by the reference isodose; $TV_{RI,i}$, target volume covered by the *i*th reference dose; $V_{CO,i}$, OAR volume; $V_{COref,i}$, OAR volume receiving at least the reference dose; $V(OAR)_{>tol}$, fractional volume of the OAR receiving more than a predefined tolerance dose; V_{RI}, volume of the reference isodose; $V_{RI,i}$, total isodose volume of the *i*th reference dose.

As previously mentioned, the first CI was suggested by the RTOG in 1993 (CI_{RTOG}).[14] Even though this index is easy to interpret, a false-perfect score could be acquired if the volume of V_{RI} and TV are the same, even though the shapes are different. The Saint-Anne–Lariboisière–Tenon group suggested the lesion coverage volume factor (CVF).[15] This index could not evaluate the irradiated volumes of normal tissues adjacent to the target. Lomax and Scheib[16] developed the healthy tissue CI (HTCI) to reflect the irradiation of normal tissues by the reference dose. However, this index could not provide exact information about target coverage. Leung et al[17] modified the HTCI to reflect numerous reference doses to various targets. On the other hand, the conformation number (CN) suggested by van't Riet et al[18] and Paddick[19] could reflect both the target coverage and the irradiation of normal tissues at the same time. Despite the capability of dual evaluation of the target coverage and the irradiation of normal tissue, it was not distinguishable which factor lowered the value of the CN. Baltas et al[20] suggested the COnformal INdex, which was a combination of the CN and the terms accounting for OARs. This index could not provide dissociable information either, and there were no considerations for the tolerance levels of individual OARs. To overcome this drawback, Menhel et al[21] proposed the critical organ scoring index to compare individual involvement of the OARs specifically at various dose levels. Wagner et al[22] proposed the conformity/gradient index (CGI), which is an average of the conformity score (CGI_c) and gradient score (CGI_g). The CGI_c is a value that takes into account the target conformity, similar to the CI_{RTOG}. The CGI_g takes into account normal tissue sparing using the gradient method. This indicator also failed to distinguish which factor lowered the value of CGI. Furthermore, the CGI_c displays the same limitation as the CI_{RTOG}, where a false-perfect score is given to situations where the target and reference dose have the same volume, but different shapes. Dice[23] suggested the Dice similarity coefficient that is defined as the intersection volume between the TV and the V_{RI}, divided by the mean of the volumes of the TV and the V_{RI}.[24] However, this indicator was unable to distinguish overirradiation of normal tissue from underirradiation of the TV. Wu et al[25] developed a distance-based CI named the conformity distance index (CDI). The CDI was a ratio of the undesirably irradiated volume in both the target and normal tissues to the averaged surface area of the TV and V_{RI}. If the TV was separated from the V_{RI}, the value of CDI would be the same regardless of the distance between the TV and the V_{RI}. Recently, Cheung and Law[26] proposed the CI with dose and distance incorporated, taking into account the spatial information of cold spots inside the planning TV (PTV) with various different penalties. This index was based on the assumption that the coverage of gross tumour volume (GTV) is mandatory, and the cold spots are generally tolerable if they are far from the GTV even though they are inside the PTV. Various conventional CIs are summarized in Table 1.

Various CIs have been developed since 1993.[2,13–22,25,26] Most of them are based on the calculation of the volumes of the TV and the V_{RI}[2,13–22] except for the CIs suggested by Wu et al[25] and Cheung and Law,[26] which were based on the distances. The aim of this study is to present new CIs based on the calculations of distances between the surface of the TV and the V_{RI}. First, points on three-dimensional (3D) surfaces of the TV and the V_{RI} were

Figure 1. After the centroid of the target volume (TV) was defined, equiangular lines from the centroid were generated at intervals of 1° in three-dimensional space. The points of intersection (POIs) of the TV and the equiangular lines were defined. The POIs of the volume of reference isodose (V_{RI}) and the equiangular lines were also generated (a). The distances from the centroid to the TV (D_T) and the V_{RI} (D_D) were acquired for the calculation of conformity index$_{distance}$ (CI$_{distance}$) (b).

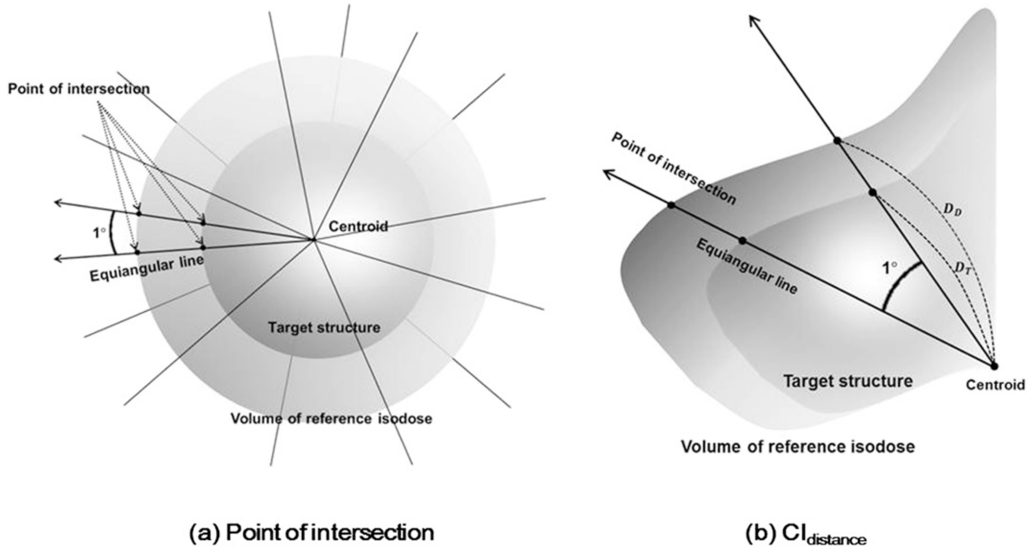

generated. Then, to evaluate not only the shape but also the target coverage, including sparing of normal tissues, the average distance between the points on the TV and the V_{RI} was calculated. The performance of the presented CIs were evaluated with virtual structures and compared with those of conventional CIs. Finally, the presented CIs were applied to the clinical prostate and head and neck (H&N) VMAT plans.

METHODS AND MATERIALS

The generation of evaluation points

An in-house program written in MATLAB® v. 8.1 (Mathworks Inc., Natick, MA), which allowed the import of TV and V_{RI} structure files in digital imaging and communications in medicine (DICOM) format was used for the calculation of CIs. The centroid of the TV was defined, then equiangular lines from the centroid were generated at intervals of 1° in 3D space. The points on the TV and V_{RI} surfaces intersecting with the equiangular lines were defined (Figure 1). When generating the equiangular lines, we first used spherical co-ordinates to define the points of intersection (POIs). We then converted the co-ordinates of the POIs into Cartesian co-ordinates. Since the TV and V_{RI} structures in DICOM format were voxelized, sometimes the equiangular lines passed between the points of the structures, thus the POI could not be defined. In this case, we took the three points from the surface structure that were closest to the equiangular line and evaluated the equiangular line intersected with the triangle formed by the points. If the equiangular line did not intersect with the triangle, we formed another triangle by searching for the next closest point and evaluated whether or not the equiangular line intersected with the new triangle. When the equiangular line intersected the triangle, we defined a plane containing the triangle. We then acquired a point at the intersection of the equiangular and the defined plane. Generally, one POI per line was generated for convex-shaped structures and two POIs were generated for concave-shaped structures, since the centroid of the concave-shaped structure was located outside the structure. The POIs of the prostate and H&N VMAT plans are shown in Figure 2.

Conformity index based on distance (conformity index$_{distance}$ and conformity index$_{abs_distance}$)

The CI by an analysis of the distances between the surface of the TV and the V_{RI} was named CI$_{distance}$. D_T and D_D were defined as the distance from the centroid to the POI on the TV and V_{RI}, respectively (Figure 1). The CI$_{distance}$ was calculated as follows:

$$\mathrm{CI}_{\mathrm{distance}} = \frac{\sum_{i=1}^{N} \frac{D_D - D_T}{D_T}}{N} \times 100 \quad (1)$$

In a similar way, the CI$_{distance}$ using the absolute value of the differences in distance was calculated and named CI$_{abs_distance}$, which was calculated as follows:

$$\mathrm{CI}_{\mathrm{abs\_distance}} = \frac{\sum_{i=1}^{N} \frac{|D_D - D_T|}{D_T}}{N} \times 100 \quad (2)$$

Both the CI$_{distance}$ and CI$_{abs_distance}$ become 0 when the TV and V_{RI} were matched perfectly. Larger values of CI$_{distance}$ and CI$_{abs_distance}$ indicate worse conformity. The standard deviations (SDs) of the CI$_{distance}$ and CI$_{abs_distance}$ were also calculated. Since D_T was the denominator in Equations (1) and (2), if D_T was 0, which meant the centroid was located at the surface of the TV, both CI$_{distance}$ and CI$_{abs_distance}$ became infinity. Therefore, CI$_{distance}$ and CI$_{abs_distance}$ could not be applied when the centroid was located at the surface of the TV. This is a limitation of the presented CIs.

Figure 2. The points of intersection (POIs) between the equiangular lines and the target volume (TV) surface are shown with black dots, while the POIs between the equiangular lines and the surface of volume of reference isodose (V_{RI}) are shown with grey dots. POIs from the prostate volumetric-modulated arc therapy (VMAT) plans (a) and the head and neck VMAT plans (b) are shown.

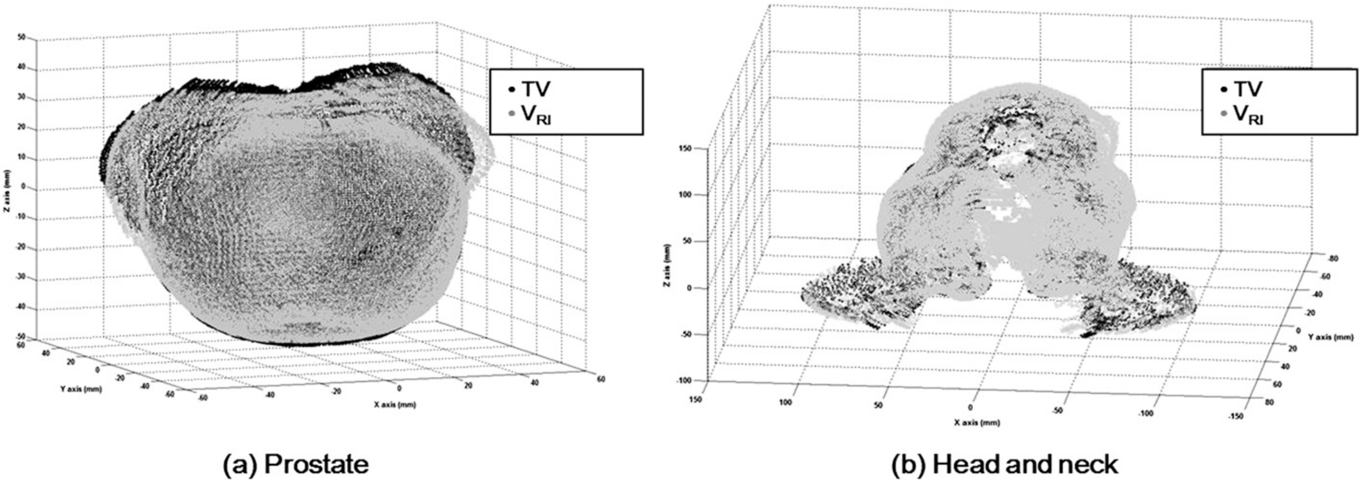

The equations can be applied to the convex-shaped structure as it is. However, for the concave-shaped structure, the centroid could be located outside of the TV. In order to resolve this situation, we considered several cases (Figure 3). The general rules were (1) if there were two POIs on the surface of the TV or V_{RI}, the larger values of D_D and D_T were taken for analysis. (2) If there was no POI at the TV, a new line in the opposite direction to the original equiangular line was generated and evaluated. (3)

Figure 3. Various situations where the equiangular lines intersect with the surface of the target volume (TV) and the volume of the reference isodose (V_{RI}) are illustrated. The first case is that the concave-shaped TV is covered fully by the V_{RI} (a). The second case is that the concave-shaped TV is covered partially by the V_{RI} (b). The situation of the concave-shaped TV covered fully by the V_{RI} and the centroid located inside the V_{RI} at the same time are shown (c). The last case is that the convex-shaped TV is covered fully by the V_{RI} (d).

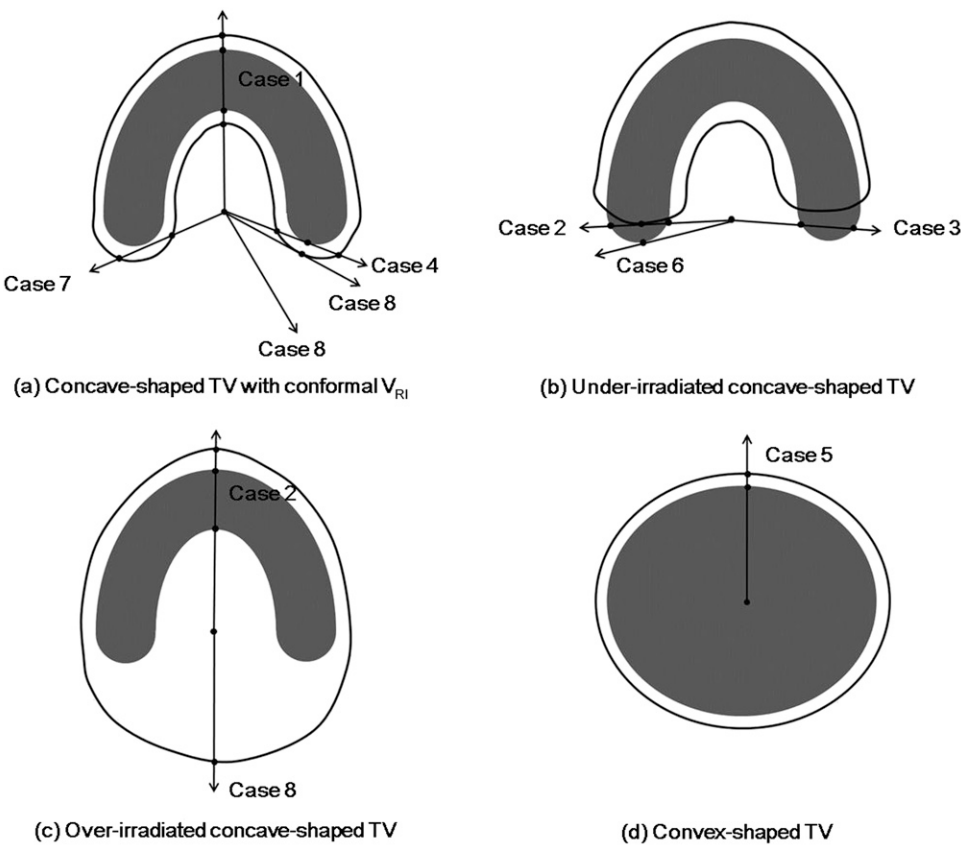

Figure 4. The virtual structures to evaluate the performances of the presented conformity indices are illustrated. The structures were a sphere-shaped (a), cubic-shaped (b), teardrop-shaped (c) and concave-shaped (d) structure. The volumes of all the structures were 500 cm^3. a, side of a cubic-shaped structure; h, height of a cone that is a component of a teardrop-shaped structure; l, length of a concave-shaped structure; r, radius of a hemisphere; R, radius of a sphere-shaped structure; r_1, inner radius of a concave-shaped structure; r_2, outer radius of a concave-shaped structure.

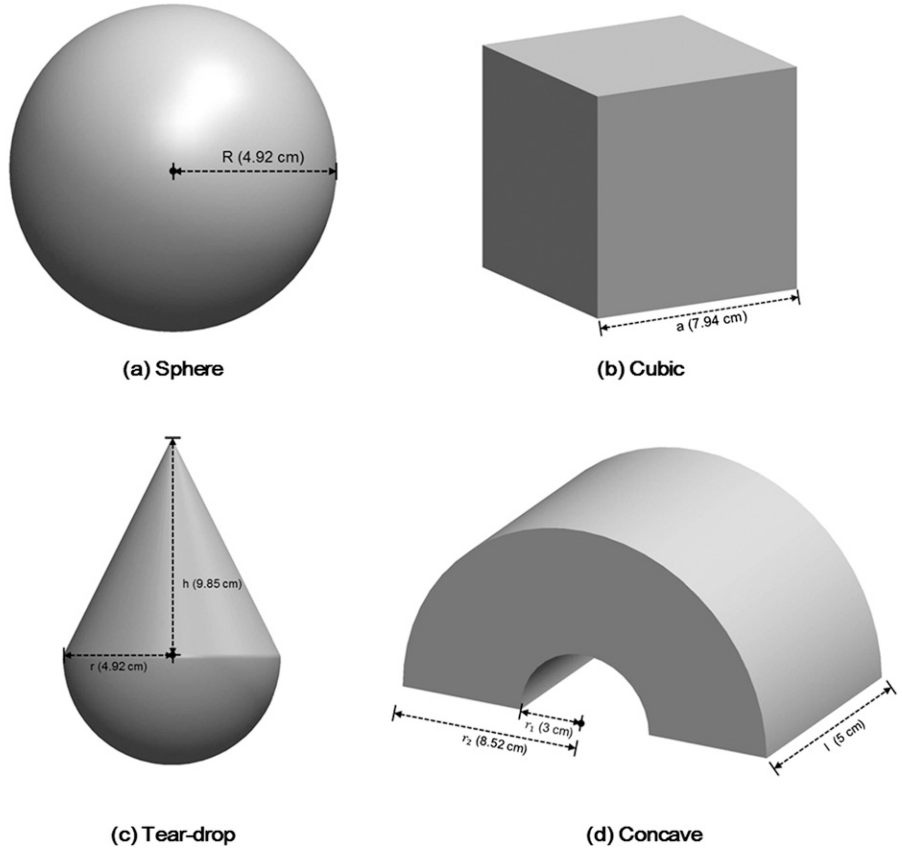

If the new line in the opposite direction had two POIs on the surface of the TV or V_{RI}, the smaller values of D_D and D_T were taken. (4) If there were two POIs at the TV and no POI at the V_{RI}, the larger value at the TV was taken as D_T and the smaller value at the TV was taken as D_D. In this case, the value of the difference had a minus sign, which induced that $CI_{distance}$ had a minus sign since the target coverage was insufficient. (5) If there were no POIs at the TV and two POIs at the V_{RI}, the larger value at the V_{RI} was taken as D_D and the smaller value at the V_{RI} was taken as D_T, which induced a plus sign of $CI_{distance}$ since the target coverage was sufficient. With these general rules, we could resolve the situation assumed in Figure 3.

Performance evaluations of the presented CIs with virtual structures

The performance of the presented CIs were evaluated with virtual structures and compared with conventional CIs. The virtual structures used were a sphere, cubic structure, teardrop-shaped structure and concave-shaped structure (Figure 4). Each structure had a volume of 500 cm^3.

For each structure, a total of six situations were analysed (Figure 5). The situations included a perfect match, an expansion of the distance from the centroid to the V_{RI} compared with the distance from the centroid to the TV by 10% (named 10% increase), a reduction of the distance from the centroid to the V_{RI} compared with the distance from the centroid to the TV by 10% (named 10% decrease), a lateral shift of the V_{RI} by 3 cm, a rotation of the V_{RI} by 45° and a spherical-shaped V_{RI} with the same volume as the TV. In the case of the sphere, the situation of the rotation and the spherical-shaped V_{RI} were not performed since there were no differences. The conventional CIs as well as the $CI_{distance}$ and the $CI_{abs\_distance}$ were calculated in these situations and compared with one another.

Performance evaluations of the presented CIs with structures from the prostate and the head and neck plans

The presented indices were applied to the TV and V_{RI} in real cases. The TV and V_{RI} from five prostate and five H&N VMAT plans were exported in DICOM format and then imported into the in-house program. The isodoses of the prescription doses that were 50.4 Gy for prostate VMAT plans and 54 Gy for H&N VMAT plans were selected as reference isodoses, respectively. The prostate VMAT plans were generated using TrueBeam™ STx with high-definition multileaf collimator (MLC) (Varian Medical Systems, Palo Alto, CA), while the H&N VMAT plans were generated using Trilogy™ with Millennium

Figure 5. A total of six situations to compare the performances of the presented conformity indices are illustrated. The situations were a perfect match (a), an expansion of the distance from the centroid to the volume of reference isodose (V_{RI}) compared with the distance from the centroid to the target volume (TV) by 10% (b), a reduction by 10% (c), a 3-cm lateral shift of V_{RI} (d), a 45° rotation of V_{RI} (e) and a spherical-shaped V_{RI} with the same volume as the TV (f). The TV and the V_{RI} are delineated with solid and dashed lines, respectively.

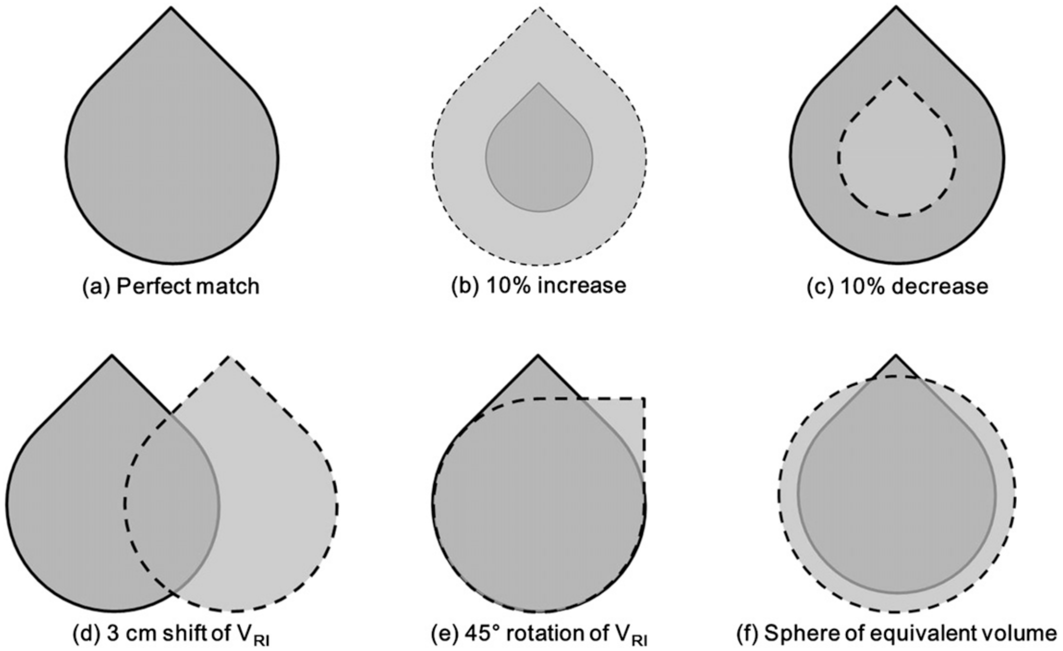

120™ MLC (Varian Medical Systems) in the Eclipse™ system (Varian Medical Systems). Not only the $CI_{distance}$ and $CI_{abs\_distance}$ but also conventional CIs were calculated for those structures. The performance of the $CI_{distance}$ and $CI_{abs\_distance}$ were evaluated by a manual review of dose distributions calculated on CT images slice by slice and compared with conventional CIs.

RESULTS

Results with the virtual structures

The values of $CI_{distance}$ and $CI_{abs\_distance}$ with conventional CIs are listed in Table 2. In the situation of the perfect match, the $CI_{distance}$ and $CI_{abs\_distance}$ were 0 with SDs of 0 in every structure, which were perfect scores. The conventional CIs also showed perfect scores in every structure.

In the situation of 10% increase, the values of $CI_{distance}$ and $CI_{abs\_distance}$ were near 10 with SDs of near 0. Similarly, in the situation of 10% decrease, the values of $CI_{distance}$ and $CI_{abs\_distance}$ were near −10 and 10 with SDs of near 0, respectively. Theoretically, the values of $CI_{distance}$ and $CI_{abs\_distance}$ should be exactly 10 or −10, not near 10 or −10. In addition, their SDs should be exactly 0. However, the quantization effect due to the voxelized grids of the structures made for some uncertainties in the results, hence the SDs were near 0 and not exactly 0. The value of CI_{RTOG} was 1.33 in the situation of the 10% increase, indicating that the volume of V_{RI} was larger than the volume of TV by as much as 33%. In the situation of the 10% decrease, the value of CI_{RTOG} was 0.73, indicating that the volume of V_{RI} was smaller than the volume of TV by as much as 27%. The CVF showed a false-perfect score for the 10% increase, while the HTCI showed a false-perfect score for the 10% decrease. The value of CVF in the situation of the 10% decrease was similar to the value of the HTCI in the situation of the 10% increase, which were 0.73 and 0.75, respectively. The values of CN in both the situations of the expansion and reduction were almost the same as each other. Similarly, the values of CDI in both the situations of expansion and reduction were also almost the same as each other. Neither the CN nor the CDI make it possible to distinguish the situation of unnecessary irradiation of normal tissue from the situation of underirradiation of the TV by a prescription dose.

When shifting the V_{RI} by 3 cm, the values of $CI_{distance}$ were almost 0 with SDs ranging from 24 to 31. The values of $CI_{abs\_distance}$ were >15 with SDs >16 in every structure. The CI_{RTOG} showed a false-perfect score in this situation. Since the non-overlapped volumes of the TV and the V_{RI} were the same in the situation of shifting, the value of CVF was the same as the value of HTCI.

In the case of rotation, the values of the $CI_{distance}$ were near 0 with SDs >16. The values of $CI_{abs\_distance}$ ranged from 13 to 23 with SDs >11. The CI_{RTOG} showed a false-perfect score. Similar to the situation of shifting, the non-overlapped volumes of the TV and the V_{RI} were the same when rotating the structure, therefore, the value of CVF was the same as the value of HTCI.

In the situation of the equivalent sphere, the values of $CI_{distance}$ ranged from −7 to 15 while those of $CI_{abs\_distance}$ ranged from 11 to 15. The CI_{RTOG} also showed a false-perfect score in this situation.

Table 2. The conformity index $(CI)_{distance}$ and $CI_{abs\_distance}$ with conventional CIs calculated at various situations with virtual structures

Situation	Mean ± standard deviation		Conventional CI				
	$CI_{distance}$	$CI_{abs\_distance}$	CI defined by Radiation Therapy Oncology Group	Coverage volume factor	Healthy tissue CI	Conformation number	Conformity distance index (cm)
Sphere							
Perfect match	0.00 ± 0.00	0.00 ± 0.00	1.00	1.00	1.00	1.00	0
10% increase[a]	10.00 ± 0.02	10.00 ± 0.02	1.33	1.00	0.75	0.75	0.49
10% decrease[b]	−10.00 ± 0.02	10.00 ± 0.02	0.73	0.73	1.00	0.73	0.49
Shift (3 cm)[c]	0.17 ± 31.34	26.1 ± 17.35	1.00	0.56	0.56	0.31	1.45
Cubic							
Perfect match	0.00 ± 0.00	0.00 ± 0.00	1.00	1.00	1.00	1.00	0
10% increase	10.00 ± 1.26	10.00 ± 1.26	1.33	1.00	0.75	0.75	0.40
10% decrease	−9.99 ± 0.54	9.99 ± 0.54	0.73	0.73	1.00	0.73	0.40
Shift (3 cm)	0.07 ± 30.50	15.39 ± 26.33	1.00	0.62	0.62	0.39	1.00
Rotation (45°)[d]	0.02 ± 16.73	12.65 ± 11.15	1.00	0.83	0.83	0.69	0.45
Equivalent sphere[e]	3.15 ± 12.50	11.1 ± 6.54	1.00	0.84	0.84	0.71	0.46
Teardrop-shaped structure							
Perfect match	0.00 ± 0.00	0.00 ± 0.00	1.00	1.00	1.00	1.00	0.00
10% increase	10.00 ± 0.5	10.05 ± 0.50	1.33	1.00	0.75	0.75	0.46
10% decrease	−10.03 ± 0.75	10.03 ± 0.75	0.73	0.73	1.00	0.73	0.46

(Continued)

Table 2. (Continued)

Situation	Mean ± standard deviation		Conventional CI				
	$CI_{distance}$	$CI_{abs\_distance}$	CI defined by Radiation Therapy Oncology Group	Coverage volume factor	Healthy tissue CI	Conformation number	Conformity distance index (cm)
Shift (3 cm)	0.05 ± 28.90	18.02 ± 24.81	1.00	0.51	0.51	0.26	1.51
Rotation (45°)	0.02 ± 20.15	19.47 ± 15.48	1.00	0.87	0.87	0.77	0.39
Equivalent sphere	−7.11 ± 15.83	14.79 ± 9.08	1.00	0.92	0.92	0.85	0.26
Concave-shaped structure							
Perfect match	0.00 ± 0.00	0.00 ± 0.00	1.00	1.00	1.00	1.00	0.00
10% increase	10.01 ± 0.34	10.01 ± 0.34	1.33	1.00	0.75	0.75	0.37
10% decrease	−10.00 ± 0.11	10.00 ± 0.11	0.73	0.73	1.00	0.73	0.32
Shift (3 cm)	0.01 ± 23.50	15.79 ± 16.48	1.00	0.66	0.66	0.43	0.78
Rotation (45°)	0.02 ± 31.91	22.67 ± 18.01	1.00	0.75	0.75	0.56	0.57
Equivalent sphere	8.10 ± 24.12	15.09 ± 21.11	1.00	0.21	0.21	0.04	2.14

[a]10% increase = the increase of the $CI_{distance}$ by 10%.
[b]10% decrease = the decrease of the $CI_{distance}$ by 10%.
[c]Shift (3 cm) = the lateral shift of volume reference isodose (V_{RI}) by 3 cm.
[d]Rotation (45°) = the rotation of V_{RI} by 45°.
[e]Equivalent sphere = spherical-shaped V_{RI} with same volume as the target volume.

Results with the structures from the prostate and the head and neck volumetric modulated arc therapy plans

The values of the $CI_{distance}$ and $CI_{abs\_distance}$ with their SDs are listed in Table 3. All the CIs calculated from the prostate VMAT plans showed lower values with lower SDs than those from the H&N VMAT plans. The average values of the $CI_{distance}$ and $CI_{abs\_distance}$ in the prostate plans were 0.13 ± 7.44 and 4.71 ± 5.81, respectively. The average values were 6.04 ± 23.27 and 10.98 ± 15.19 in the H&N plans, respectively. In prostate plans, CI_{RTOG} ranged from 0.97 to 1.02, while CI_{RTOG} ranged from 1.86 to 2.38 in the H&N plans. The CVF and HTCI ranged from 0.92 to 0.94 in the prostate plans. In the H&N plans, the CVF showed almost perfect scores while the HTCI ranged from 0.42 to 0.53. The values of the CN were relatively low in the H&N plans compared with the prostate plans owing to the low values of HTCI. The average value of the CDI was 0.44 cm in the prostate plans and 1.59 cm in the H&N plans. Among the five prostate VMAT plans, the value of $CI_{distance}$ from Plan 1 showed the best score, which was the closest value to 0, while $CI_{distance}$ from Plan 3 showed the worst score, which was the largest absolute value with the largest value of SD. Among the five H&N VMAT plans, the $CI_{distance}$ from Plan 1 was the best, while the $CI_{distance}$ from Plan 4 was the worst. The TV and V_{RI} of prostate Plans 1 and 3 at the representative axial CT slice are shown in Figure 6, while those of the H&N Plans 1 and 4 are shown in Figure 7.

DISCUSSION

The values of $CI_{distance}$ and $CI_{abs\_distance}$ can provide useful information when they are used in combination with their SDs. When both the values of $CI_{distance}$ and $CI_{abs\_distance}$ and their SDs were 0, it indicated a perfect match of the TV and the V_{RI}. The $CI_{distance}$ and $CI_{abs\_distance}$ make possible the evaluation not only of the congruence in shape between the TV and the V_{RI} but also the degree of the target coverage and the sparing of normal tissue. If the values of $CI_{distance}$ and $CI_{abs\_distance}$ were not 0 and their SDs were 0, this indicated a perfect match only in shape but not in size between the TV and V_{RI}. The $CI_{abs\_distance}$ does not give information about the target coverage. On the other hand, the $CI_{distance}$ with a plus sign indicated that the V_{RI} generally exceeded the TV, which means the irradiation of normal tissue by the reference dose, while a minus sign indicated that the prescription dose was not delivered to the whole volume of the target. If the shape and size of the underdosed volume in the target were the same as those of the overdosed volume of normal tissue, and the centroid was located in the overlapped region between the TV and V_{RI}, then the value of $CI_{distance}$ was near 0 owing to the distances with plus signs were cancelled out by the distances with the minus signs irrespective of the target coverage. However, in this situation, the SD of $CI_{distance}$ was not 0, which was 0 in the perfect match. Therefore, this kind of mismatch could be identified when there is a large SD.

The CI_{RTOG} showed a false-perfect score when the volume of the TV and the V_{RI} were the same. When the TV was included in the V_{RI}, the CVF also resulted in a false-perfect score, since CVF is a ratio of the volume of the TV covered by the V_{RI} to the volume of the TV. If the TV is included in the V_{RI}, the numerator becomes the same as the denominator, and the CVF becomes one, a perfect score. Similar to this, the HTCI showed a false-perfect score when the V_{RI} was included in the TV. The CN and the CDI did not distinguish the 10% decrease from the 10% increase showing similar values to each other. On the other hand, the $CI_{distance}$ combined with the value of SD made it possible to distinguish the differences in all situations and never showed a false-perfect score in the situations analysed in this study.

When applying the presented CIs to the prostate and the H&N VMAT plans, the CIs of the prostate plans were smaller than those of the H&N plans, which indicated better conformity. This was reasonable since the conformities of the prostate plans were generally better than the H&N plans as shown in Figures 6 and 7. To review the results of the prostate plans, Plan 1 showed the best score in $CI_{distance}$, while Plan 3 showed the worst score. By a manual review of each CT slice, we concluded that the conformity of Plan 1 was slightly better than that of Plan 3, as shown in Figure 6. However, the CVF, CN and CDI showed better scores in Plan 3 than in Plan 1, which was not true. The CI_{RTOG} and HTCI showed better results in Plan 1 than in Plan 3. The CI_{RTOG} indicated that the volume of V_{RI} was larger than that of TV in Plan 3 compared with Plan 1. Furthermore, the HTCI was closer to 1 in Plan 1 than in Plan 3, which indicated that the normal tissue irradiation was higher in Plan 3 than in Plan 1. These results were congruent with the result of $CI_{distance}$ which was −0.24 in Plan 1, indicating that the average distance from the centroid of TV to the surface of TV was generally smaller than the average distance from the centroid to the surface of V_{RI} by 0.24%. In Plan 3, the value of $CI_{distance}$ was 1.89, which means that the volume of V_{RI} generally exceeds the volume of TV resulting in irradiation of normal tissue adjacent to the target by the prescribed dose. The CVF indicated that the target coverage was better in Plan 3 than in Plan 1. This was also congruent with the result of $CI_{distance}$, since the value of $CI_{distance}$ was relatively large in Plan 3 compared with Plan 1 with a plus sign. However, the differences of the conventional CIs as well as the presented CIs were not large enough to induce clinical significance. Even though we concluded that Plan 1 was slightly better than Plan 3 in terms of target conformity, the differences were negligible. In Plan 5, the value of $CI_{distance}$ had a plus sign although the value of CVF was 0.92, which means that the whole volume of TV was not covered by the V_{RI}. Therefore, the users should keep in mind that $CI_{distance}$ does not always provide the exact information about the target coverage. Since $CI_{distance}$ is an average value, it is able to show the overall tendency when the V_{RI} exceeds the TV or vice versa. The plus sign of $CI_{distance}$ does not always indicate full coverage of the TV by the V_{RI}.

To review the results of the H&N plans, Plan 1 showed the best score in $CI_{distance}$, while Plan 4 showed the worst score. We also observed slightly better conformity in Plan 1 than in Plan 4 by a manual review of CT slices as shown in Figure 7. The values of CVF, HTCI and CN from Plan 1 were the same as the values of Plan 4 even though the conformity of Plans 1 and 4 were not the same. The CDI showed better conformity in Plan 1 than in Plan 4, showing congruence with the results of $CI_{distance}$. On the contrary, CI_{RTOG} indicated that the volume of V_{RI} was 2.37 times larger than the volume of TV in Plan 1, while the V_{RI} was 2.34 times larger than the TV in Plan 4. Since the CVF and HTCI indicated that the TV was included in the V_{RI}, and the

Table 3. The conformity index $(CI)_{abs\_distance}$ and $CI_{distance}$ with conventional CIs calculated from volumetric-modulated arc therapy plans for prostate and head and neck (H&N) cancer

Plan number	$CI_{distance}$	$CI_{abs\_distance}$	CI defined by Radiation Therapy Oncology Group	Coverage volume factor	Healthy tissue CI	Conformation number	Conformity distance index (cm)
Prostate							
1	−0.24 ± 6.60	4.29 ± 5.02	0.99	0.92	0.93	0.85	0.22
2	−0.85 ± 5.88	4.13 ± 4.27	0.97	0.92	0.94	0.86	0.20
3	1.89 ± 9.98	5.93 ± 8.24	1.02	0.94	0.92	0.87	0.20
4	−0.65 ± 8.27	5.06 ± 6.57	1.01	0.92	0.92	0.85	0.83
5	0.52 ± 6.46	4.15 ± 4.97	0.98	0.92	0.94	0.86	0.73
Average	0.13 ± 7.44	4.71 ± 5.81	0.99	0.92	0.93	0.86	0.44
H&N							
1	5.14 ± 22.10	10.15 ± 18.05	2.37	1.00	0.42	0.42	1.64
2	6.48 ± 33.56	11.11 ± 20.15	2.07	0.99	0.48	0.47	1.42
3	5.48 ± 16.48	8.50 ± 10.08	1.86	0.99	0.53	0.53	1.39
4	6.99 ± 25.05	13.10 ± 15.11	2.34	1.00	0.42	0.42	1.71
5	6.11 ± 19.15	12.05 ± 12.55	2.38	0.99	0.42	0.42	1.79
Average	6.04 ± 23.27	10.98 ± 15.19	2.20	0.99	0.46	0.45	1.59

Figure 6. The axial CT slices showing target conformities in the prostate volumetric modulated arc therapy (VMAT) plans are shown. The target volume (TV) and the volume of reference isodose (V_{RI}) are delineated with inner and outer lines, respectively. A total of five prostate VMAT plans were investigated, with plan 1 showing the best score of conformity index$_{distance}$ ($CI_{distance}$) which was -0.24 ± 6.60 (a) and plan 3 showing the worst score of $CI_{distance}$ with a value of -1.89 ± 9.98 (b) is shown. A better match in shape at plan 1 than in plan 3 can be identified.

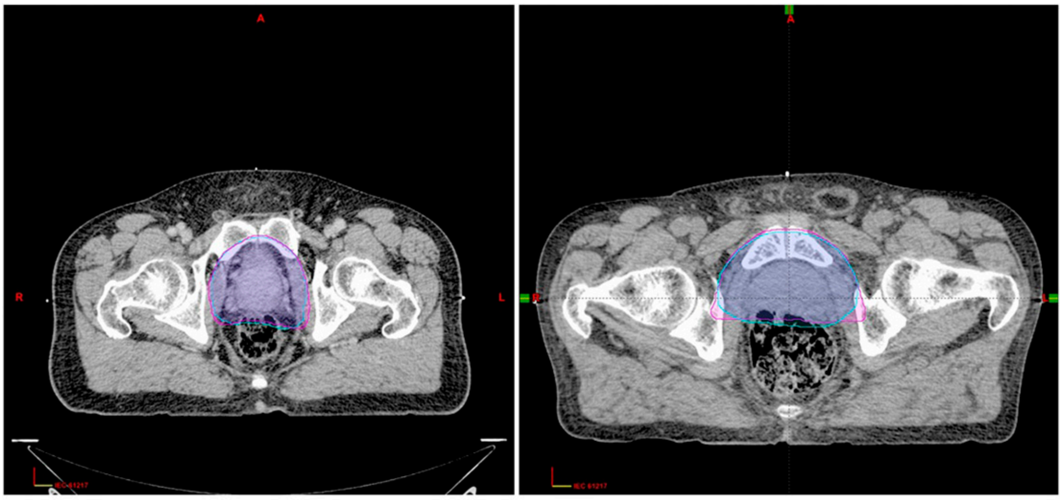

(a) TV and V_{RI} of prostate plan 1 **(b) TV and V_{RI} of prostate plan 3**

CDI and the $CI_{distance}$ indicated that the V_{RI} was larger than the TV in Plan 4 than in Plan 1, the value of CI_{RTOG} seems contradictory to the results of the other CIs. This is because the CI_{RTOG} is a ratio value between the TV and V_{RI}. The absolute volume of TV and V_{RI} were larger in Plan 4 (1421.4 cm^3 of V_{RI} and 606.2 cm^3 of TV) than in plan 1 (1206 cm^3 of V_{RI} and 507.9 cm^3 of TV). This resulted in the contradictory value of CI_{RTOG}. In the H&N plans, the differences between Plans 1 and 4 were also not significant.

Since the POIs in this study were defined at the equiangular lines from the centroid of the TV, the resolution of the POI could vary according to the volume of TV or V_{RI}. However, even for a large sphere-shaped TV, which has a diameter of 20 cm, the interval between the adjacent POIs is <1.8 mm, since the interval between each equiangular line was 1°. Although the resolution of POI was dependent on the volume of TV or V_{RI}, we believe that the resolution would be fine enough to evaluate the conformity even for a large volume of TV or V_{RI} in the clinic.

Figure 7. The axial CT slices showing target conformities in the head and neck volumetric modulated arc therapy (VMAT) plans are shown. The target volume (TV) and the volume of reference isodose (V_{RI}) are delineated with inner and outer lines, respectively. A total of five head and neck VMAT plans were investigated, with Plan 1 showing the best score of the conformity index$_{distance}$ ($CI_{distance}$) that was 5.14 ± 22.10 (a) and Plan 4 showing the worst score of $CI_{distance}$ with a value of 6.99 ± 25.05 (b). A better match in shape at Plan 1 than in Plan 4 can be identified.

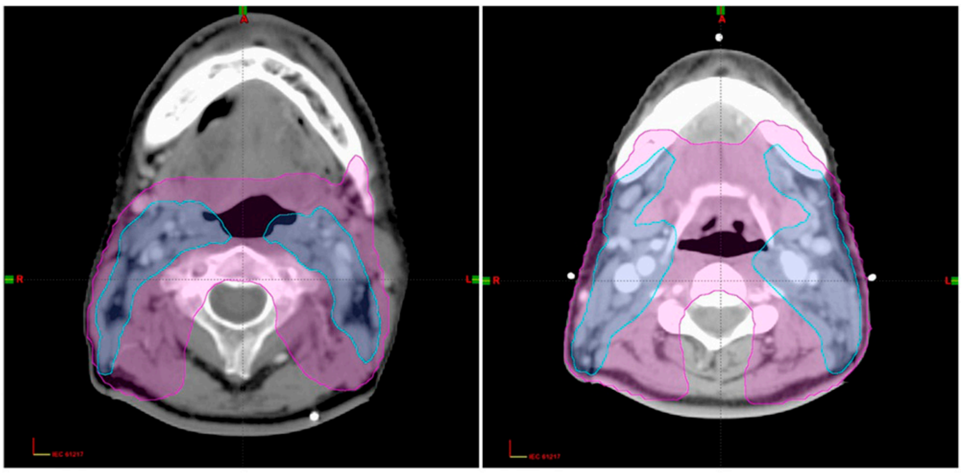

(a) TV and V_{RI} of head and neck plan 1 **(b) TV and V_{RI} of head and neck plan 4**

Every conventional CI gave specific information on the target conformity according to its own definition. On the other hand, the presented $CI_{distance}$ was able to give more comprehensive information than the conventional CIs. However, the limitation of the presented CIs was that they could not be applied when the centroid was located on the surface of the TV. Another limitation of the presented CIs was that these were incomplete to provide full information on target conformity unless these were combined with the values of SDs. An evaluation with two variables would be more confusing than that with a single variable and this was a limitation of the presented CIs. In addition, the maximum number of POIs per equiangular line for a single structure was assumed to be two in this study, therefore, when the equiangular line intersects with the surface of the structure three or more times, the presented CIs could not be used. We assumed these situations, where the centroid was located exactly at the surface of the TV or the number of POIs per equiangular line for a single structure was more than or equal to three, would rarely occur in the clinic. Even though some uncertainties existed in the presented CIs owing to the quantization effect of the voxelized grid of the structures, it was not difficult to evaluate the target conformity with the presented CIs since this uncertainty was <1.3%, as shown in the results. The appropriate values of $CI_{distance}$ and $CI_{abs\_distance}$ in the clinic were not investigated in this study and are left for future investigation.

CONCLUSION

The $CI_{distance}$ and $CI_{abs\_distance}$ based on the analysis of the distances between the TV and the V_{RI} were presented and evaluated in this study. The $CI_{distance}$ with SD demonstrated better performance than the $CI_{abs\_distance}$. When the conventional CIs resulted in false-perfect scores in some situations, $CI_{distance}$ combined with SD did not show a false-perfect score. The $CI_{distance}$ makes it possible to evaluate the target conformity comprehensively, considering not only the target coverage but also the irradiation of normal tissue adjacent to the target by the prescribed dose. However, it does not always provide the exact information about target coverage or irradiation of normal tissue since the $CI_{distance}$ is an average value. It is able to show the overall tendency when the V_{RI} exceeds the TV or vice versa.

FUNDING

This work was supported by the Interdisciplinary Research Initiatives Program by the College of Engineering and College of Medicine, Seoul National University (2013), Seoul, Republic of Korea.

REFERENCES

1. Sung W, Park JM, Choi CH, Ha SW, Ye SJ. The effect of photon energy on intensity-modulated radiation therapy (IMRT) plans for prostate cancer. *Radiat Oncol J* 2012; **30**: 27–35. doi: 10.3857/roj.2012.30.1.27
2. Feuvret L, Noel G, Mazeron JJ, Bey P. Conformity index: a review. *Int J Radiat Oncol Biol Phys* 2006; **64**: 333–42.
3. Kim JY, Park SY, Lee DH, Lee SH, Kim TH, Cho KH. Comparison of treatment plans with multileaf collimators of different leaf width. *K J Med Phys* 2001; **15**: 173–8.
4. Webb S. The physical basis of IMRT and inverse planning. *Br J Radiol* 2003; **76**: 678–89.
5. Intensity-Modulated Radiation Therapy Collaborative working Group. Intensity-modulated radiotherapy: current status and issues of interest. *Int J Radiat Oncol Biol Phys* 2001; **51**: 880–914.
6. Chen AM, Farwell DG, Luu Q, Vazquez EG, Lau DH, Purdy JA. Intensity-modulated radiotherapy is associated with improved global quality of life among long-term survivors of head-and-neck cancer. *Int J Radiat Oncol Biol Phys* 2012; **84**: 170–5. doi: 10.1016/j.ijrobp.2011.11.026
7. Kam MK, Chau RM, Suen J, Choi PH, Teo PM. Intensity-modulated radiotherapy in nasopharyngeal carcinoma: dosimetric advantage over conventional plans and feasibility of dose escalation. *Int J Radiat Oncol Biol Phys* 2003; **56**: 145–57.
8. Quan EM, Li X, Li Y, Wang X, Kudchadker RJ, Johnson JL, et al. A comprehensive comparison of IMRT and VMAT plan quality for prostate cancer treatment. *Int J Radiat Oncol Biol Phys* 2012; **83**: 1169–78. doi: 10.1016/j.ijrobp.2011.09.015
9. Otto K. Volumetric modulated arc therapy: IMRT in a single gantry arc. *Med Phys* 2008; **35**: 310–17.
10. Fenkell L, Kaminsky I, Breen S, Huang S, Van Prooijen M, Ringash J. Dosimetric comparison of IMRT *vs* 3D conformal radiotherapy in the treatment of cancer of the cervical esophagus. *Radiother Oncol* 2008; **89**: 287–91. doi: 10.1016/j.radonc.2008.08.008
11. Wolff D, Stieler F, Welzel G, Lorenz F, Abo-Madyan Y, Mai S, et al. Volumetric modulated arc therapy (VMAT) *vs* serial tomotherapy, step-and-shoot IMRT and 3D-conformal RT for treatment of prostate cancer. *Radiother Oncol* 2009; **93**: 226–33. doi: 10.1016/j.radonc.2009.08.011
12. Lee YK, Bedford JL, McNair HA, Hawkins MA. Comparison of deliverable IMRT and VMAT for spine metastases using a simultaneous integrated boost. *Br J Radiol* 2013; **86**: 20120466. doi: 10.1259/bjr.20120466
13. International Commission on Radiation Units and Measurements. *Prescribing, recording, and reporting photon beam therapy.* Bethesda, MD: ICRU; 1999.
14. Shaw E, Kline R, Gillin M, Souhami L, Hirschfeld A, Dinapoli R, et al. Radiation therapy oncology group: radiosurgery quality assurance guidelines. *Int J Radiat Oncol Biol Phys* 1993; **27**: 1231–9.
15. Lefkopoulos D, Grandjean P, Platoni K. Progress in optimizing dosimetry plans in stereotactic radiotherapy in the salt group. [In French.] *Cancer Radiother* 1998; **2**: 127–38.
16. Lomax NJ, Scheib SG. Quantifying the degree of conformity in radiosurgery treatment planning. *Int J Radiat Oncol Biol Phys* 2003; **55**: 1409–19.
17. Leung LH, Kan MW, Cheng AC, Wong WK, Yau CC. A new dose-volume-based Plan Quality Index for IMRT plan comparison. *Radiother Oncol* 2007; **85**: 407–17.
18. van't Riet A, Mak AC, Moerland MA, Elders LH, van der Zee W. A conformation number to quantify the degree of conformality in brachytherapy and external beam irradiation: application to the prostate. *Int J Radiat Oncol Biol Phys* 1997; **37**: 731–6.
19. Paddick I. A simple scoring ratio to index the conformity of radiosurgical treatment plans. Technical note. *J Neurosurg* 2000; **93**(Suppl. 3): 219–22.

20. Baltas D, Kolotas C, Geramani K, Mould RF, Ioannidis G, Kekchidi M, et al. A conformal index (COIN) to evaluate implant quality and dose specification in brachytherapy. *Int J Radiat Oncol Biol Phys* 1998; **40**: 515–24.
21. Menhel J, Levin D, Alezra D, Symon Z, Pfeffer R. Assessing the quality of conformal treatment planning: a new tool for quantitative comparison. *Phys Med Biol* 2006; **51**: 5363–75.
22. Wagner TH, Bova FJ, Friedman WA, Buatti JM, Bouchet LG, Meeks SL. A simple and reliable index for scoring rival stereotactic radiosurgery plans. *Int J Radiat Oncol Biol Phys* 2003; **57**: 1141–9.
23. Dice LR. Measures of the amount of ecologic association between species. *Ecology* 1945; **26**: 297–302.
24. Nielsen MH, Berg M, Pedersen AN, Andersen K, Glavicic V, Jakobsen EH, et al. Delineation of target volumes and organs at risk in adjuvant radiotherapy of early breast cancer: national guidelines and contouring atlas by the Danish Breast Cancer Cooperative Group. *Acta Oncol* 2013; **52**: 703–10. doi: 10.3109/0284186X.2013.765064
25. Wu QR, Wessels BW, Einstein DB, Maciunas RJ, Kim EY, Kinsella TJ. Quality of coverage: conformity measures for stereotactic radiosurgery. *J Appl Clin Med Phys* 2003; **4**: 374–81.
26. Cheung FW, Law MY. A novel conformity index for intensity modulated radiation therapy plan evaluation. *Med Phys* 2012; **39**: 5740–56. doi: 10.1118/1.4742848